

# Matrix and Temperature Effects on the Electronic Properties of Conjugated Molecules: An Electroabsorption Study of *all-trans*-Retinal

Sarah A. Locknar, Arindam Chowdhury, and Linda A. Peteanu\*

Department of Chemistry, Carnegie Mellon University, Pittsburgh, Pennsylvania 15213

Received: November 8, 1999; In Final Form: March 9, 2000

Using Stark effect (electroabsorption) spectroscopy to study *all-trans*-retinal (ATR) in a variety of polymer matrices and organic glasses, we have found that the average change in polarizability upon excitation ( $\overline{\Delta\alpha}$ ) that we measure is highly dependent on the rigidity of the matrix used. In rigid polymer and organic glass matrices, the measured values of  $\overline{\Delta\alpha}$  are in the range of 20–50 Å<sup>3</sup> and those calculated using semiempirical methods are in the range of 60–85 Å<sup>3</sup>. In contrast,  $\overline{\Delta\alpha}$ 's that are up to an order of magnitude higher are measured when the ATR is entrained in nonrigid polymer matrices such as those that are above their glass-transition temperature, or those containing trapped solvent. We have postulated that large values of  $\overline{\Delta\alpha}$  may be the result of field-induced orientation of ATR within polymer matrices that are not fully rigid. The  $|\Delta\mu|$  of ATR ranges from roughly 3 to 11 D, depending on the polarity and the rigidity of the environment. In addition, vibrational structure is apparent in the electroabsorption spectra of ATR in methylcyclohexane and methyltetrahydrofuran glasses at 77 K that is assigned to a progression of the C=C stretch.

## Introduction

Retinal is a common photopigment in nature (Figure 1) found in the proteins rhodopsin and bacteriorhodopsin (bR). *All-trans*-retinal, which is the focus of this study, is found in bR where it is linked to the protein via a protonated Schiff base.<sup>1</sup> A problem of recurring interest in the study of these protein systems is the origin of the opsin shift.<sup>2</sup> This is the absorption shift that occurs between retinals in solution and those bound to the protein and between various color-sensitive visual pigments. There are a number of interactions that are considered to be important in bringing about the opsin shift.<sup>3</sup> These include extension of  $\pi$  conjugation of retinal due to increased planarity in the protein cavity and interactions of the retinal with charged and/or polarizable amino acid residues or other counterions in the protein cavity. Both experiments and calculations have suggested that the latter mechanism could contribute substantially to the magnitude of the opsin shift.<sup>3</sup> Evaluating the contribution of these interactions requires data on the changes in dipole moment,  $|\Delta\mu|$ , and in polarizability,  $\overline{\Delta\alpha}$ , of the retinal upon excitation. Because both the  $|\Delta\mu|$  and  $\overline{\Delta\alpha}$  of retinal are sensitive to the polarity and polarizability of its environment, comparing the values measured in matrices of varying polarity to those obtained in the protein itself would give insight into the dielectric properties of the protein cavity. This approach has been employed to probe the local fields of proteins and membrane structures using naturally-occurring carotenoids and synthetic voltage-sensitive dyes.<sup>4–6</sup>

The retinals and bR have also received considerable attention in the realm of nonlinear optics due to their relatively large hyperpolarizabilities ( $\beta$ ).<sup>7–9</sup> While the value of  $\beta$  is linked to  $\Delta\mu$  by the well-known two-state approximation,<sup>10</sup>  $\overline{\Delta\alpha}$  has also been predicted to contribute substantially to both the value of  $\beta$  and its variation with solvent polarity.<sup>11,12</sup>

The motivation for this study is to address the discrepancy found in retinals between the large values of  $\overline{\Delta\alpha}$  that have

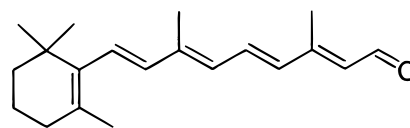


Figure 1. Structure of *all-trans*-retinal.

been measured by Stark-effect spectroscopy<sup>13–15</sup> ( $\overline{\Delta\alpha}^{\text{Stark}}$ ) compared to those predicted via semiempirical calculations.<sup>16,17</sup> The quantity that is calculated is the electronic  $\overline{\Delta\alpha}^{\text{el}}$  of the molecule, which we designate as  $\overline{\Delta\alpha}^{\text{el}}$ . In retinals, values of  $\overline{\Delta\alpha}^{\text{Stark}}$  in the range of 300–1500 Å<sup>3</sup> have been measured by electroabsorption spectroscopy,<sup>13–15</sup> while calculated values are between 50 and 100 Å<sup>3</sup>.<sup>13,16</sup> A discrepancy of similar size was noted in the case of several donor–acceptor (D–A) polyenes.<sup>16,18,19</sup> In contrast, quite good agreement is seen between the measured and calculated values of  $\overline{\Delta\alpha}$  in short-chain nonpolar (unsubstituted) diphenylpolyenes.<sup>13,16,20,21</sup> This marked difference in the results for polar and nonpolar systems suggested the possibility that field-induced orientation of the ATR and/or of the polar groups of the matrices may make a substantial contribution to the value of  $\overline{\Delta\alpha}^{\text{Stark}}$ . This would represent an *orientational*  $\overline{\Delta\alpha}$  that, along with the intrinsic  $\overline{\Delta\alpha}^{\text{el}}$  of the molecule, contributes to the value of  $\overline{\Delta\alpha}^{\text{Stark}}$  that is measured here. This model suggests that, when the orientational contribution is minimal,  $\overline{\Delta\alpha}^{\text{Stark}}$  may be identified with  $\overline{\Delta\alpha}^{\text{el}}$ , resulting in a greatly improved agreement between measured and calculated values of  $\overline{\Delta\alpha}$ . We define the relationship between  $\overline{\Delta\alpha}^{\text{Stark}}$  and  $\overline{\Delta\alpha}^{\text{el}}$  more explicitly in the Experimental Section and in the Appendix to this paper.

The results obtained in this work have led us to explore the role played by the matrix itself in the measurement of  $\overline{\Delta\alpha}$  via electroabsorption. A common method of performing Stark spectroscopy involves using an isotropic distribution of probe molecules in a rigid polymer matrix<sup>13,14,22,23</sup> or in an organic or

aqueous glass.<sup>19,24,25</sup> The assumption of rigidity plays an important role in the analysis of the data. In order to obtain  $\Delta\alpha^{\text{el}}$  from an electroabsorption spectrum, one must assume that there is no field-induced alignment of the molecules of interest or of the matrix itself. However, the evidence we present below and in ref 26 suggests that there can be residual mobility of a dopant molecule even within a polymer that is below its glass transition temperature ( $T_g$ ). Such mobility may be linked to the decay in the bulk value of the nonlinear optical hyperpolarizability that has been observed due to loss of alignment of the chromophores in poled polymers.<sup>27</sup>

In this paper, we investigate the rodlike substituted polyene, ATR, which has a ground-state dipole moment between 3 and 5.5 D.<sup>21,28–31</sup> In ref 26 we used coumarin 153 (C153) which is a disk-shaped molecule with a ground-state dipole moment of 6.5 D<sup>32,33</sup> as our probe molecule. Both studies show that only organic glasses and some polymer glasses at temperatures well below their respective  $T_g$ 's provide a rigid enough matrix upon which to perform accurate electroabsorption measurements.<sup>26</sup> In such matrices, we obtain values of  $\Delta\alpha^{\text{Stark}}$  for ATR and other probes<sup>26</sup> that are in good agreement with the results of finite-field<sup>34,35</sup> calculations. Interestingly, the values of  $\Delta\alpha^{\text{Stark}}$  that we report here for ATR in the rigid polymer matrices ( $\sim 50 \text{ \AA}^3$ ) and optical glasses ( $\sim 20 \text{ \AA}^3$ ) are similar to those measured by Ponder and Mathies (20–90  $\text{ \AA}^3$ ) for the ATR protonated Schiff base (PSB) in the protein bR contained in vesicles in a matrix of poly(vinyl alcohol) at 77 K.<sup>36</sup> A comparison with our results suggests that ATR-PSB is contained in a fairly rigid cavity within the protein.

A useful consequence of the derivative nature of Stark-effect spectroscopy is that the vibrational structure within a molecular absorption spectrum is highlighted. This has the remarkable effect of revealing the vibrational structure underlying the absorption spectrum of ATR, which is nearly structureless even at 1.8 K in an EPA (ethyl ether:isopentane:ethanol 5:5:2, v/v) matrix.<sup>37</sup> This structure is assigned to a progression of the C=C stretch and is similar to that seen by El-Sayed and co-workers in hole burning studies of bR.<sup>38</sup>

## Experimental Section

**Sample Preparation.** ATR, poly(methyl methacrylate) (PMMA), poly(vinyl chloride) (PVC), and dichloroethane (Aldrich) were used without further purification. Polystyrene (PS) was a gift from Dr. Matyjaszewski and was used as received. 2-Methyltetrahydrofuran (MeTHF, Acros) and methylcyclohexane (MCH, Aldrich) were used immediately after refluxing under Ar atmosphere over  $\text{CaH}_2$  for at least an hour to remove water. All samples were prepared and handled under dim red light.

Polymer films of PMMA, PS, and PVC were made by dissolving ATR and the desired polymer together in dichloroethane, pouring the mixture into an aluminum dish, and evaporating the solvent. Films were then either glued between ITO (indium tin oxide)-coated slides with a viscous solution of PMMA in dichloroethane and left to dry for 24 h,<sup>13</sup> or clamped between the slides and heated in a 150 °C oven for 5 min and then used immediately. Heating did not alter the absorbance maximum of the ATR in the films, indicating that there was no substantial thermal isomerization or degradation of the ATR. PE films were prepared by swelling the films in a chloroform solution containing ATR at a millimolar concentration. After at least 30 min, the films were removed, allowed to air-dry, and heated between ITO slides as described above. In the cast films (PMMA, PS, and PVC) the final absorbance of the sample

was 0.3–0.8, and in the PE films it was  $\sim 0.1$ . We saw no additional peaks in the absorption spectra of any of the samples which would indicate aggregation of the ATR molecules. To obtain an accurate measure of the film thickness, an interference pattern of fringes was measured in the 900–2500 nm range using a UV–vis–near-IR absorption spectrometer (Perkin-Elmer Lambda 900) as described previously.<sup>13</sup> This interference method gave a standard deviation in the thickness of 1.5–10  $\mu\text{m}$  depending on the uniformity of the polymer film. Since this was the major source of error in our measurements on the polymer films, an average weighted by the standard deviation of the thickness was used to determine  $\Delta\alpha^{\text{Stark}}$  and  $|\Delta\mu|$  and the standard deviation in these parameters.<sup>39</sup> The measurements were repeated a minimum of three times on different sample preparations. To perform measurements at low temperature on the PE films, the sample was placed in contact with a coldfinger which in turn was in contact with a liquid nitrogen ( $\text{LN}_2$ ) reservoir within an optical vacuum dewar (Janis model SD138). Temperatures of the sample routinely reach 150–200 K with this system.

The organic glasses were prepared with a roughly 0.05 M solution of ATR in pure dried solvents. The final absorbance of the samples were 0.2–0.8. As before, no new features appeared in the absorption spectrum of ATR at low temperature versus room temperature solution. This confirms that the ATR did not aggregate in the glasses. The solution was placed into a well created with Kapton tape ( $\sim 25 \mu\text{m}$  thick) applied to an ITO-coated glass slide. Another ITO-coated slide was pressed onto the first (with the coated sides of the glass facing each other) and held together with spring clips. The entire sample cell was then immersed in a  $\text{LN}_2$  optical dewar (H. S. Martin). The thickness of the cells were determined by the interference pattern described above.

Electroabsorption spectra were obtained with a home-built spectrometer which has been described previously.<sup>13</sup> In essence, it consists of a 150 W xenon arc lamp, 0.3 M single monochromator, horizontal polarizer, and photodiode detector which is connected to a lock-in amplifier. A high-voltage ac power supply is used to deliver  $\sim 10^6$  V/cm to the sample via the optically transparent ITO electrodes at a frequency of  $\sim 450$  Hz. The power supply also provides the reference frequency for phase-sensitive light detection in the lock-in amplifier.

**Theory of Electroabsorption and Data Fitting.** The theory behind electroabsorption was developed by Liptay<sup>40</sup> and is summarized here with some slight changes in formalism. The overall change in transmitted light intensity caused by the application of an electric field is described by the following equation:<sup>41</sup>

$$-\left(\frac{2\sqrt{2}}{2.303}\right)\frac{\Delta I}{I} = \Delta A(v) = \mathbf{F}^2 \left[ a_{\chi} A(v) + b_{\chi} \frac{v}{h} \frac{\partial}{\partial v} \left( \frac{A(v)}{v} \right) + c_{\chi} \frac{v}{h^2} \frac{\partial^2}{\partial v^2} \left( \frac{A(v)}{v} \right) \right] \quad (1)$$

The  $\Delta I/I$  term is a measure of the intensity change as a result of the applied field normalized to the total light intensity reaching the detector. Both  $\Delta I$  and  $I$  were measured simultaneously by the lock-in amplifier, using the locked ( $\Delta I$ ) and total voltage ( $I$ ) channels. The factor of  $2\sqrt{2}$  is needed to convert from rms voltage (read in by the lock-in amplifier) to an equivalent dc voltage, and the factor of 2.303 is derived from Beer's law. The  $A(v)$  represents the unperturbed absorption as a function of frequency,  $\mathbf{F}$  represents the field at the sample in V/cm, and  $h$  is Planck's constant. The subscript  $\chi$  represents

the angle between the direction of the applied electric field and the electric field vector of the polarized light. The expressions for  $a_\chi$ ,  $b_\chi$ , and  $c_\chi$  are given below for the magic angle ( $\chi = 54.7^\circ$ ).

$$a_{54.7} = \frac{1}{30|\mathbf{m}|^2} \sum_{ij} 10A_{ij}^2 + \frac{1}{15|\mathbf{m}|^2} \sum_{ij} 10\mathbf{m}_i \mathbf{B}_{ij} + \frac{\beta}{15|\mathbf{m}|^2} \sum_{ij} 10\mathbf{m}_i A_{ij} \mu_{gj} \quad (2)$$

$$b_{54.7} = \frac{10}{|\mathbf{m}|^2} \sum_{ij} \mathbf{m}_i A_{ij} \Delta\mu_j + \frac{15}{2} \overline{\Delta\alpha^{\text{el}}} + 5\beta(\mu_g \cdot \Delta\mu) \quad (3)$$

$$c_{54.7} = 5|\Delta\mu|^2 \quad (4)$$

The symbols  $\alpha$  and  $\mu$  represent the polarizability and dipole moment, respectively. The  $\Delta$  signifies the change between the ground and excited-state properties of the molecule. A bar indicates the average (i.e.,  $\overline{\Delta\alpha^{\text{el}}} = 1/3 \text{Tr}(\overline{\Delta\alpha^{\text{el}}})$ ) and the indices  $i$  and  $j$  label the vector/tensor components along  $x$ ,  $y$ , and  $z$ . The transition moment is represented by  $\mathbf{m}$  and the tensors  $\mathbf{A}$  and  $\mathbf{B}$  represent the transition polarizability and hyperpolarizability respectively, as a result of the effect of the applied electric field on the molecular transition moment:  $\mathbf{m}(F) = \mathbf{m} + \mathbf{A} \cdot F + F \cdot \mathbf{B} \cdot F$ . These terms account for the effect of the applied field on the transition moment.

The expression for  $\overline{\Delta\alpha^{\text{el}}}$  (eq 3) requires further comment. Note that the fit to the experimental electroabsorption spectrum gives  $b_{54.7}$  which we identify as the measured value  $\overline{\Delta\alpha^{\text{Stark}}}$  in this work. In order to equate  $\overline{\Delta\alpha^{\text{Stark}}}$  with  $\overline{\Delta\alpha^{\text{el}}}$  alone, we must make two assumptions. One is to neglect the transition moment polarizability, thereby eliminating the first term in eq 3. One can regard the transition moment polarizability as a higher-order correction to  $\overline{\Delta\alpha^{\text{el}}}$ . Neglect of this term is justifiable because sizable field effects on transition moments are normally seen only in forbidden transitions, not in strongly allowed  $\pi-\pi^*$  transitions such as that of ATR. We recognize that field-induced mixing of the  $1B_u$  and the low-lying  $2A_g$  state in ATR might conceivably cause a change in  $\mathbf{m}$  which could cause the first term in eq 3 to be an important contribution to the magnitude of  $\overline{\Delta\alpha^{\text{Stark}}}$ . However, we can invoke several arguments to support our neglect of this term. The first is that, if  $\mathbf{A}$  were to be large, this would be evident as a significant  $a_{54.7}$  term. However, the values of  $a_{54.7}$  obtained from the fitting of the data are very small in the rigid matrices (on the order of  $10^{-16}$ – $10^{-17} \text{ cm}^2/\text{V}^2$ ) and *negative*. Moreover, symmetry arguments can be used to predict that  $\mathbf{A}$  will be much smaller than  $\mathbf{B}$  so that the dominant contribution to  $a_{54.7}$  should arise from  $\mathbf{B}$  rather than  $\mathbf{A}$  (eq 2).<sup>19</sup> Also, to our knowledge, no solvent polarity effects on the extinction coefficient of ATR have been reported. This suggests that the electric-field effect on the transition moment will be small, also justifying our neglect of the first term in eq 3.

The second assumption we must make is to neglect the term containing the Boltzmann prefactor,  $\beta = 1/kT$ . This term arises in Liptay's formation for the field-induced molecular orientation to first order. Neglect of this term is valid if the ATR molecules are isotropically distributed in a rigid environment and therefore cannot reorient on the time scale of the oscillating applied electric field. In essence, a fixed isotropic distribution corresponds to a very high temperature ( $\beta \sim 0$ ), *regardless* of the actual temperature of the sample because the molecular dipoles

remain random even in the presence of an aligning field. One focus of this paper is to determine whether or not this approximation is valid for polar molecules in polymer and organic frozen glasses.

The  $c_{54.7}$  term describes the interaction of the molecular dipole moment with the applied field. For a system in which an equal number of molecules are aligned parallel and antiparallel to the applied field, this causes a broadening of the absorption spectrum if  $\Delta\mu$  is not zero. The difference between the broadened spectrum and the unperturbed spectrum results in a line shape that is the second derivative of the unperturbed absorption spectrum. Note that  $c_{54.7}$  does not contain terms with the Boltzmann prefactor. Nonetheless, we have found that the magnitude of  $|\Delta\mu|$  also depends on the rigidity and temperature of the matrix. However, as shown below, the effect of these matrix properties is far less dramatic on  $|\Delta\mu|$  than on  $\overline{\Delta\alpha^{\text{Stark}}}$ .

**Calculations.** The geometry of ATR was optimized using AM1.<sup>42</sup> The resulting geometry was similar to that obtained from analysis of the crystal structure.<sup>16,43</sup> To calculate the changes in properties between the ground ( $1A_g$ ) and one-photon allowed ( $2B_u$ ) electronic states in ATR, we have used a MNDO/SCI method for the calculation of  $\Delta\mu$ ,<sup>13</sup> and, as described in ref 16, an INDO/SCI/FF method for the calculation of  $\overline{\Delta\alpha^{\text{el}}}$  at fixed molecular geometry. The gas-phase calculations were then corrected for solvation as described previously,<sup>13,44</sup> using both Onsager-type reaction fields<sup>40</sup> and cavity fields for an elliptical cavity.<sup>45</sup> The solvent-corrected values are designated  $\Delta\alpha_{\text{calc}}$  and  $\Delta\mu_{\text{calc}}$ . For the organic glasses, we have used room temperature values for the refractive index ( $n$ ) and dielectric constants ( $\epsilon_0$ ). Work by Sakurai et al.<sup>46</sup> has demonstrated that the interaction between ATR and solvents is adequately modeled by continuum theory, at least in the solution phase. Whether this holds for molecules in polymers or glasses is the subject of current research.<sup>47</sup> It should be noted here that the continuum solvent model assumes a fixed molecular geometry. It does *not* account for possible solvent-induced changes in the C=C and C–C bond lengths. However, as explained later in the text, we do not expect this to be a significant limitation for retinal.

The gas-phase value for  $\Delta\mu$  was found to be 4.6 D using MNDO/SCI. In contrast, the INDO/SCI method yielded a  $\Delta\mu$  of 9.3 D in the gas phase, which is similar to the value of 8.9 D reported by Hendrickx et al.<sup>7</sup> Addition of solvent corrections to the  $\Delta\mu$  calculated by INDO/SCI increased it to within the range of 14–18.5 D, which is much larger than our experimental values. For this reason, these are not included in Table 1.

Good agreement is seen between the gas-phase value of  $\Delta\alpha$  calculated with the INDO/SCI/FF method ( $39.5 \text{ \AA}^3$ ) and that from a higher level INDO/MRD/SDCI sum-over-states method ( $32 \text{ \AA}^3$ ),<sup>48</sup> as we have found in the past.<sup>16</sup> Because, of the two methods, only INDO/MRD/SDCI is able to properly model the  $2A_g$  states of polyenes, agreement between the results of the two methods for ATR and for other polyenes<sup>16</sup> suggests that the observed mixing of the  $2A_g$  state into the  $1B_u$  in ATR<sup>49</sup> may not make a large contribution to the value of  $\overline{\Delta\alpha}$  in these systems. This hypothesis is further supported by the good agreement that is obtained for *nonpolar polyenes* between the calculated<sup>16</sup> and experimental values<sup>21,36</sup> of  $\overline{\Delta\alpha}$ .

## Results and Discussion

**Electroabsorption Spectra and Fits.** In all cases, the electroabsorption spectra are fit nicely by a single set of parameters (Figures 2 and 3). The measured and calculated values of  $\Delta\mu$  and  $\overline{\Delta\alpha}$  of ATR and the absorption maxima ( $\lambda_{\text{max}}$ ) in all the matrices studied here are summarized in Table

**TABLE 1: Electroabsorption Results of ATR in Various Matrices<sup>a</sup>**

	$n$	$\epsilon$	$T_g^b$	$f^2 \overline{\Delta\alpha}^{\text{Stark}}$	$\overline{\Delta\alpha}_{\text{calc}}^c$	$f \Delta\mu $	$\Delta\mu_{\text{calc}}^d$	$\lambda_{\text{max}}^e$
glued PMMA <sup>f</sup>	1.44	10.7		$342 \pm 22$	82	$11.0 \pm 0.4$	8.3	375
PMMA	1.49	3.9	378	$52 \pm 2$	73	$8.5 \pm 0.2$	7.6	377
PVC	1.54	3.5	354	$43 \pm 2$	72	$9.6 \pm 0.3$	7.5	391
PS	1.59	2.49	373	$30 \pm 7$	67	$6.2 \pm 0.8$	7.1	382
PE	1.51	2.26	148	$724 \pm 146$	64	$2.7 \pm 0.9$	6.8	374
PE(77 K)	1.58	2.27	148	$37 \pm 10$	65	$4.5 \pm 2.3$	6.9	381
MCH(77 K)	1.42	2.0	87 <sup>g</sup>	$27 \pm 10$	61	$10.4 \pm 0.8$	6.5	385
MeTHF(77 K)	1.41	4.6	91 <sup>h</sup>	$33 \pm 10$	74	$10.7 \pm 1.0$	7.6	389

<sup>a</sup> Polarizabilities are reported in  $\text{\AA}^3$  and dipole moments in debyes (D). <sup>b</sup> Units in kelvin. Taken from ref 73 unless otherwise noted. These are glass-transition temperatures for pure solvents. <sup>c</sup> Errors are  $\pm 3 \text{\AA}^3$  as determined from an estimated error of 10% in the cavity volume. <sup>d</sup> Calculated with MNDO (see Experimental Section section) Errors are  $\pm 0.3$  D as determined from an estimated error of 10% in the cavity volume. <sup>e</sup> Measured in nm. Errors are approximately  $\pm 2$  nm. <sup>f</sup> These samples were prepared by gluing the PMMA film between electrodes using a dichloroethane/PMMA solution (see Experimental Section). Solvent corrections here were done for a solvent of dichloroethane. <sup>g</sup> See ref 64. <sup>h</sup> See ref 74.

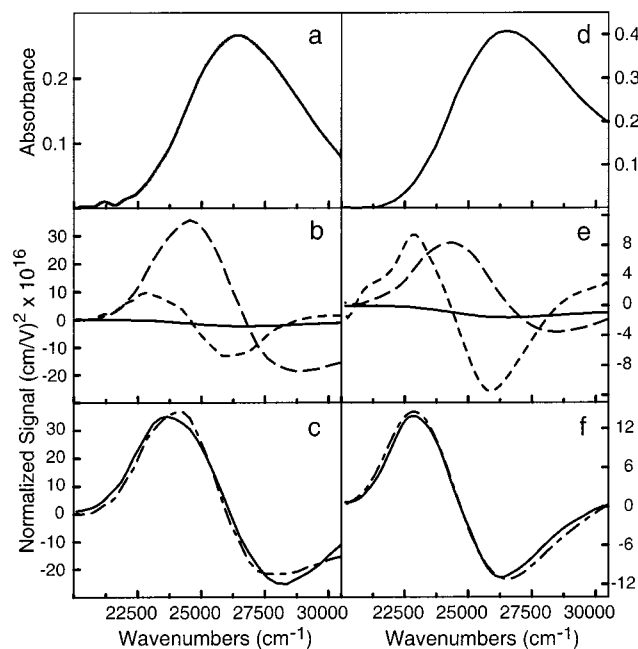


**Figure 2.** Electroabsorption of ATR at 298 K in PMMA which has been glued (a–c) and heated (d–f) between the electrodes. Top: Absorption spectra Middle: Zeroth (solid), first (dashed), and second (dotted) derivative components of the fit. Bottom: Electroabsorption spectrum (solid) and fit (dashed–dot) at  $\chi = 54.7^\circ$ . The glued sample has been reproduced from an earlier work.<sup>13</sup>

1. In Figure 2 we depict the spectra obtained from two PMMA samples prepared by different methods. Glued PMMA samples (Figure 2a–c) refer to those that have been dried by evaporation and which may contain residual dichloroethane (see Experimental Section). The electroabsorption spectrum of ATR in this matrix is broad and featureless (Figure 2c)<sup>13,14</sup> and the fit contains a substantial first derivative ( $\overline{\Delta\alpha}^{\text{Stark}}$ ) contribution (Figure 2b). On the right-hand side of Figure 2 are spectra obtained in PMMA samples that were heated prior to the electroabsorption measurement (see Experimental Section). This causes a marked decrease in the first derivative contribution to the fit (Figure 2e). As a result, there is a 4-fold decrease in  $\overline{\Delta\alpha}^{\text{Stark}}$  while  $|\Delta\mu|$  (the second derivative contribution to the fit) decreases by less than 20%. The electroabsorption spectra of ATR in all of the other polymer samples that are below their glass transition temperatures (PS, PVC, and PE at 77 K) are broad and unstructured and are similar to the spectrum shown in Figure 2f.

Unlike the electroabsorption spectra of ATR in the polymer films described above, the spectra in the organic glasses MCH

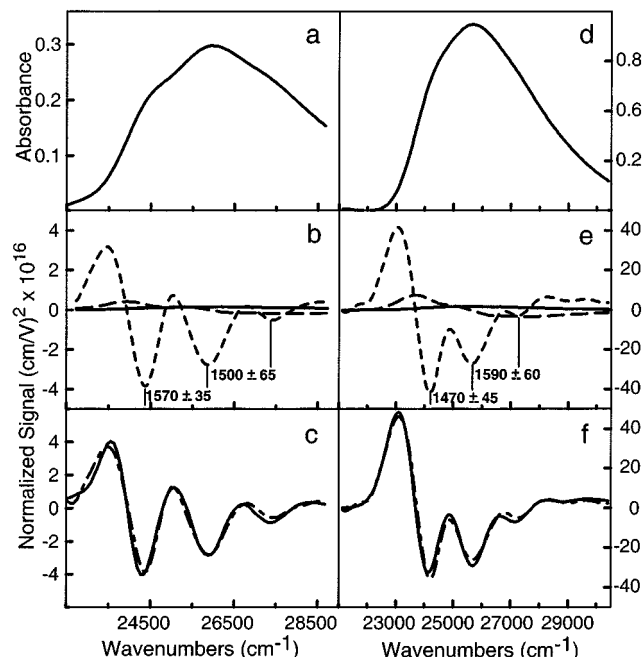


**Figure 3.** Electroabsorption spectrum and fit of ATR at 77 K in methylcyclohexane (a–c) and in methyl THF (d–f) at  $\chi = 54.7^\circ$ . The top two spectra (a and d) represent the absorption spectra. In b and e are depicted the zeroth (solid), first (dashed), and second (dotted) derivative components of the fit. The vibrational separations are indicated in  $\text{cm}^{-1}$ . The bottom spectra (c and f) show the electroabsorption spectra (solid) and the fits (dashed–dot).

and MeTHF (Figure 3) exhibit a fair amount of structure that is indicative of a more ordered local environment. These features, attributable to a vibronic progression in the excited state, will be discussed in greater detail later. The electroabsorption spectra in these matrices are clearly dominated by the second derivative of the absorption spectrum ( $|\Delta\mu|$ ) which is also reflected in the small values of  $\overline{\Delta\alpha}^{\text{Stark}}$  extracted from the fit (Table 1). The spectra are fit well by a single set of parameters, indicating that the dipolar properties do not vary substantially with vibrational excitation as has been seen in other polyene systems.<sup>19,20,50</sup>

**Matrix Polarity.** In order to rationalize the dramatic effect of the matrix on the dipolar properties of ATR described above, we must consider what effect lowering the temperature of the matrix (PE, MeTHF, MCH) or heating (PMMA) of the matrix may have on its polarity. For this, we refer to the values of the absorption maxima ( $\lambda_{\text{max}}$ ) that have been compiled in Table 1. Considering first the solvent glasses, recent results in the literature suggest that the effective polarities of organic glasses

are enhanced by the presence of polar solutes.<sup>47</sup> This study of thermochromism in the absorption spectra of solvatochromic dyes in various organic glasses has indicated that the polarity of the probe molecule greatly influences the effective polarity of the frozen environment.<sup>47</sup> In fact, the temperature-dependent shifts in  $\lambda_{\max}$  in MCH and MeTHF glasses were shown to be nearly identical for a given probe molecule.<sup>47</sup> In the experiments reported here, it appears as though the *relative* polarities in these two environments remain nearly the same at 298 K versus 77 K, though the *absolute* polarity of each may be substantially increased at low temperature. An increase in dielectric constant ( $\epsilon_0$ ) in the glasses may also rationalize the nearly identical values of  $|\Delta\mu|$  measured in the two matrices. An increase in  $\epsilon_0$  for both matrices would increase both  $\Delta\mu_{\text{calc}}$  and  $\Delta\alpha_{\text{calc}}$  and cause their predicted values in the two environments to become more similar.<sup>51</sup> Both of these effects would enhance the agreement between experiment and calculation in the organic glass matrices (Table 1).

Considering now the polarity of the polymer environments, we have also observed that cooling the PE sample to 77 K shifts the  $\lambda_{\max}$  of ATR from 374 to 381 nm (Table 1). We first considered that the shift was caused by an increase in local polarity of the PE matrix with decreased temperature, as seen in the glasses described above. Such an increase in polarity could be due, potentially, to an increase in the crystallinity of the environment at low temperature.<sup>52</sup> However, we see no increase in cloudiness of our films upon cooling that would suggest a greater crystallinity of the films at low temperature. Moreover, we failed to see a temperature-dependent shift in  $\lambda_{\max}$  for the solvatochromic probe molecule coumarin 153 in a PE matrix.<sup>19</sup> We next considered the possibilities of contraction of the cavity around ATR upon cooling and an increase in planarity (and conjugation) of ATR as the result of interactions with the matrix. We expect the effect of cavity contraction to be relatively small based on estimates of the solvation corrections with varying cavity size.<sup>53</sup> Therefore, we believe that the increase in  $\lambda_{\max}$  upon cooling is likely due to an increase in planarity of the ATR in PE. This does not, however, preclude the contribution of other effects. In contrast to what is observed for PE, we find that glued and heated PMMA have  $\lambda_{\max}$  values that are only 2 nm different. This indicates that the local environment of the ATR and/or its degree of planarity are quite similar in both.

In the following section, we shall evaluate the predictive ability of the calculations of  $\Delta\mu_{\text{calc}}$  and  $\Delta\alpha_{\text{calc}}$  for ATR in the various media studied here, and then present a model to explain the discrepancies we observe. In the final section, we will discuss the vibrational structure that is unique to the spectra obtained in the organic glass matrices.

#### Comparison of Experimental and Calculated Values.

Several clear trends that emerge on examination of the entire data set in Table 1 can be summarized as follows: (1)  $\Delta\mu_{\text{calc}}$  and  $\Delta\alpha$  vary only modestly among this wide range of matrices while significantly greater variance is seen in the experimental numbers, (2) particularly for  $\Delta\alpha$ , agreement between experiment and calculation is poor, and (3) direct correlation between the values of  $\Delta\alpha^{\text{Stark}}$  and  $|\Delta\mu|$  and matrix polarity ( $\epsilon_0$ ) appears to be weak or nonexistent. In the following discussion, we will argue that the *rigidity* of the matrices is the most important parameter determining the variation in  $\Delta\alpha^{\text{Stark}}$ , and possibly  $|\Delta\mu|$ , seen in these data.<sup>54</sup>

Focusing first on  $\Delta\alpha^{\text{Stark}}$ , the largest measured values occur in two polymers—glued PMMA and room temperature PE—which we will discuss in turn. Values of  $\Delta\alpha^{\text{Stark}}$  for retinals in

glued PMMA matrices have been measured to be on the order of 200–300 Å<sup>3</sup> by us<sup>13</sup> and by Ponder and Mathies.<sup>14</sup> We have found that heating the PMMA samples prior to the electroabsorption measurements (see Experimental Section) leads to a 4-fold decrease in  $\Delta\alpha^{\text{Stark}}$  to  $\sim 50$  Å<sup>3</sup>, bringing  $\Delta\alpha^{\text{Stark}}$  into much better agreement with  $\Delta\alpha_{\text{calc}}$  (Table 1). In contrast, heating of the sample causes a decrease in  $|\Delta\mu|$  of less than 20% and minimally alters the effective polarity of the matrix as judged by the 2 nm shift to longer wavelength of  $\lambda_{\max}$ . The other polymer samples below their  $T_g$ 's (PS, PVC, and PE at 77 K) give values of  $\Delta\alpha^{\text{Stark}}$  in the range of 25–50 Å<sup>3</sup>. These values are similar to the calculated values and to the results obtained in the heated PMMA samples (Table 1).

Turning our attention to the second matrix in which large values of  $\Delta\alpha^{\text{Stark}}$  were observed, room temperature PE,  $\Delta\alpha^{\text{Stark}}$  is on the order of 700 Å<sup>3</sup>. At the same time, a very small value of  $|\Delta\mu|$  is found that is even smaller than  $\Delta\mu_{\text{calc}}$  without addition of any solvent corrections (4.6 D). Similarly large values of  $\Delta\alpha^{\text{Stark}}$  (1000 ± 300 Å<sup>3</sup>) for ATR in room-temperature PE have also been reported by Davidsson and Johanssen, with a  $|\Delta\mu|$  of 15 D.<sup>15</sup> Again, the measured values of  $\Delta\alpha^{\text{Stark}}$  represent a substantial deviation from theoretical predictions (Table 1). We have found that lowering the temperature of the matrix to 77 K markedly decreases  $\Delta\alpha^{\text{Stark}}$ , bringing it more in line with  $\Delta\alpha_{\text{calc}}$ . In our data, there is a concomitant increase in  $|\Delta\mu|$  though there is a substantial standard deviation in this parameter in our data set.

**Orientalional Polarizability Model.** We consider here a possible model to explain the results described above. Before doing so, however, it is useful to clarify and distinguish between the effects on molecular properties due to the solvent field of the matrix environment versus those due to the externally applied field (Stark field) in the electroabsorption experiment. The solvent field considered here is due to alignment of the matrix molecules around the dipole moment of the solute and is on the order of 10<sup>7</sup> V/cm in nonpolar hydrocarbons to 10<sup>8</sup> V/cm in polar solvents. Its effect on the ground and excited-state values of the dipole moment and polarizability of the probe molecule determines the central frequency and breadth of the absorption band. In many D–A polyenes, the solvent fields are also predicted to drastically alter the ground-state structure (particularly the C=C and C–C bond lengths) and charge distribution of the probe molecule.<sup>18,19</sup> These effects will be discussed later in greater detail, but in ATR, we expect them to be small based on resonance Raman studies.<sup>55,56</sup> Though thermal energy in the matrix may cause the solvent fields to fluctuate, several experiments have predicted large ordered fields in some biological systems and surrounding polar chromophores in organic glasses.<sup>47</sup> The enhancement of  $\Delta\mu$  and  $\Delta\alpha$  relative to their gas-phase values that is due to the solvent can be estimated using the continuum models of the reaction and cavity fields (Experimental Section).

The field applied in an electroabsorption experiment (Stark field) is at least 1 order of magnitude smaller than the solvent fields described above. Nonetheless, phase-sensitive detection using a lock-in amplifier enables the small changes to the absorption spectrum caused by the oscillating Stark field to be observed over the background of a large static solvent field. The analysis of the electroabsorption spectrum is based on the assumption that the Stark field induces a *perturbation* to the absorption spectrum. For this condition to hold, the Stark field must be much smaller than any solvent fields. Therefore, we would expect  $\Delta\alpha$ ,  $|\Delta\mu|$ , and  $\lambda_{\max}$  of the probe molecule to

follow a trend with some measure of the solvent field (such as  $\epsilon_0$ ) in different matrices. The continuum model predicts that, in ATR, as  $\epsilon_0$  increases, so should  $\overline{\Delta\alpha}$ ,  $|\Delta\mu|$ , and  $\lambda_{\max}$ . However, it is clear that this trend is not present in the data reported here. Therefore, we must identify characteristics of the matrix, *other* than polarity, that could explain the variation in measured properties of ATR, and particularly in  $\overline{\Delta\alpha}^{\text{Stark}}$ . As explained below, rigidity is the matrix characteristic that appears to best correlate with the measured values of  $\overline{\Delta\alpha}^{\text{Stark}}$  for the probe molecules.

If the matrix is not fully rigid, it is reasonable to assume that the probe molecules can rotate in response to the Stark field. To visualize how a large  $\overline{\Delta\alpha}^{\text{Stark}}$  will result from orientational motion of the chromophore in the applied field, let us begin with the simplest possible model—a dipole moment in the gas phase. We will then discuss the influence of the surrounding matrix. Suppose we have a permanent ground-state dipole moment ( $\mu_g$ ) in the gas phase in an ac electric field. This dipole can orient instantaneously (on the time scale of the field fluctuation or  $\sim 500$  Hz) to its minimum energy configuration in the field. Because  $\mu_g$  orients instantaneously in the applied field, the effects on the electroabsorption spectrum of the molecule would depend on the square of the ac field (its magnitude and not its direction). In accord with the Born–Oppenheimer principle,  $\mu_e$  will not reorient in response to the field on the time scale of absorption. If  $\mu_e$  is parallel to and larger than  $\mu_g$  (as is the case in ATR), we should see a red shift of the absorption spectrum in the field or a first-derivative contribution to the Stark spectrum. This is because the excited state, with its larger  $\mu_e$ , will be stabilized more than the ground state by the matrix field. This red shift would be interpreted as the  $\overline{\Delta\alpha}^{\text{Stark}}$  in the course of electroabsorption analysis. In essence, this *is* molecular polarizability—the change in the energy of the system in response to the applied field. Of course, in a molecule such as ATR, there is also an *electronic* contribution to  $\overline{\Delta\alpha}$  that is due to the intrinsic polarizability of the electrons of the molecule. Because the value of  $\overline{\Delta\alpha}^{\text{el}}$  for ATR is positive, it also gives rise to a red shift of the absorption band in the field. Therefore, in ATR, the *effective* value of  $\overline{\Delta\alpha}^{\text{Stark}}$  obtained from the electroabsorption analysis would contain contributions from both the electronic and orientational  $\overline{\Delta\alpha}$ 's. An analogous effect is seen in studies of the frequency dependence of the Stark effect in PMMA films at temperatures above their  $T_g$ .<sup>57</sup> Liptay accounts for orientation contributions to the effective  $\overline{\Delta\alpha}^{\text{Stark}}$  with the term containing the  $\beta(1/kT)$  prefactor in eq 3.

It is important to note here that, in an actual sample, the extent of rotation is only expected to be a few degrees due to collisions with the matrix. Taking this into account, a model calculation using eq 3 shows that, for a molecule with  $\mu_g = 5$  D and a parallel  $\mu_e$  of 10 D, a rotation of  $30^\circ$  in response to a Stark field of  $5 \times 10^5$  V/cm would produce an orientational contribution to  $\overline{\Delta\alpha}^{\text{Stark}}$  of  $450 \text{ \AA}^3$ . This value is the same order of magnitude as that observed in glued PMMA and room temperature PE samples (Table 1). It is also important to point out that the electroabsorption experiment measures the *average* properties of the probe molecules. In the sample calculation above, the *average* rotation of the probe molecule is  $30^\circ$ . In reality, some probe molecules may be more free to rotate within the matrix than are others and thus have a larger orientational contribution to  $\overline{\Delta\alpha}^{\text{Stark}}$  while others may be rotating less or not at all.<sup>58</sup>

Now let us see how orientational motion of the ground-state dipole in the applied field would affect the measurement of  $|\Delta\mu|$ . In a fixed isotropic sample, the value of  $|\Delta\mu|$  is obtained by measuring the symmetric broadening (second derivative) of the absorption spectrum due to the Stark field acting on an ensemble of dipoles that are randomly oriented and fixed in space. If these dipoles can orient in the field, the distribution will no longer be isotropic. In that case, the extent of field-induced broadening on the high-energy side of the spectrum will be lessened and the  $|\Delta\mu|$  obtained from Stark effect analysis will be somewhat decreased. The net effect of rotation on the measurements of *gas-phase* dipoles, then, would be an increase in measured  $\overline{\Delta\alpha}^{\text{Stark}}$  and a decrease in  $|\Delta\mu|$  that is not fully accounted for in the analysis.

The above discussion considered only an isolated probe molecule. In reality, the probe molecules are embedded in matrices which may or may not be rigid themselves. As described above, the orientational contribution to  $\overline{\Delta\alpha}^{\text{Stark}}$  can take three forms—(1) orientation of the probe due to interactions between the Stark field and its ground-state dipole moment, (2) orientation of the matrix molecules due to interactions of the Stark field with *their* dipole moments, and (3) a combination of the two. In the first case, the probe molecule can orient in the Stark field while the matrix remains essentially fixed. This picture may best describe the situation in nonpolar matrices that should only weakly interact with the Stark field. In this case, we would expect to see an increase in the measured  $\overline{\Delta\alpha}^{\text{Stark}}$  with a concomitant decrease in  $|\Delta\mu|$ , as explained above. In the second case, there is orientation of matrix molecules while the probe molecule remains essentially fixed in space. Though rotations of the matrix dipoles are likely to be quite small, they may produce substantial changes in the solvent field surrounding the probe molecule due to their additive effect. An increase in the solvent field due to Stark field-induced rotations in the matrix would result in an *amplification* of the Stark field. This would cause concomitant increase in the *effective* values of both  $\overline{\Delta\alpha}^{\text{Stark}}$  and  $|\Delta\mu|$  obtained from analysis of the electroabsorption spectrum. The final orientational model to consider incorporates instantaneous reorientation of *both* the solvent and probe molecules in the Stark field. In polar matrices where there are potentially strong interactions between the matrix dipoles and the Stark field, this would result in a large increase in measured  $\overline{\Delta\alpha}^{\text{Stark}}$  with a smaller increase in  $|\Delta\mu|$ . Presumably, the much smaller solvent molecules or polymer pendant groups would rotate more freely than would the probe molecule.

In order to see how these models could explain the data reported here, we will first consider the results obtained in the room-temperature and 77 K PE samples. The room temperature PE samples may be explained by the first mechanism described above. Recall that lowering the temperature of the matrix dramatically reduces the  $\overline{\Delta\alpha}^{\text{Stark}}$  of ATR and increases  $|\Delta\mu|$  somewhat (Table 1). As PE is above its  $T_g$  at room temperature, the shape of the matrix cavity could change to accommodate a rotating probe molecule through bulk (alpha) relaxation processes.<sup>59,60</sup> Lowering the temperature of the PE sample below its  $T_g$  makes the matrix more rigid by eliminating those relaxation processes.<sup>59,60</sup> As a result, the motion of ATR is more restricted so that it remains randomly oriented even under the influence of the applied field. We expect that alignment of the polymer matrix is small due to the relatively low polarity of the C–H bonds. However, we cannot completely rule out this possibility.

Next we consider the PMMA samples. In the PMMA samples, the larger  $\overline{\Delta\alpha}^{\text{Stark}}$  that is seen in the glued versus the heated samples is accompanied by a somewhat larger  $|\Delta\mu|$  as well. This is opposite to our finding for ATR in PE. Therefore, in order to explain the PMMA results, we are forced to invoke one of the two other models described above. As PMMA is well below its reported  $T_g$  at room temperature, it would have been expected to provide a rigid glassy environment for electroabsorption measurements. However, our method of adhering the samples together may allow a significant number of solvent molecules to become trapped within polymer matrices by specific interactions with polymer pendant groups.<sup>61,62</sup> Dichloroethane could easily interact with the pendant esters in the PMMA matrix. The second mechanism dictates that trapped solvent molecules or the polymer pendant groups themselves reorient in response to the Stark field while ATR remains essentially fixed in space. We can estimate the expected enhancement of  $\overline{\Delta\alpha}$  and  $|\Delta\mu|$  arising from an increase in the effective field acting on the molecule by noting that an increase in  $\overline{\Delta\alpha}$  will be proportional to the square of the field while  $|\Delta\mu|$  will increase in direct proportion to the field (eqs 1–4). Therefore, for an increase in  $\overline{\Delta\alpha}$  by a factor of 6.6 (such as is seen in glued versus heated PMMA), the field would have to increase by a factor of 2.6. As a result,  $|\Delta\mu|$  would increase from 8.5 to  $\sim 22$  D. As we only see an increase in  $|\Delta\mu|$  of 2.5 D, the second orientation mechanism described above does not fully account for the results we see in glued PMMA. Instead, we believe that perhaps the probe and the matrix molecules are reorienting, but by different amounts. If the ATR molecule rotates less than the matrix pendant groups or trapped solvent molecules, the  $|\Delta\mu|$  that we measure could be smaller than we would expect from simple solvent-induced amplification of the Stark field as described above. The marked decrease in  $\overline{\Delta\alpha}^{\text{Stark}}$ , and to a lesser extent  $|\Delta\mu|$ , that occurs when the matrix is heated and then cooled back to room temperature demonstrates that driving off residual solvent or annealing of the polymer is essential to the formation of a rigid matrix.

In general, the organic glasses appear to form very rigid matrices. The absorption spectra in these matrices exhibit an increase in structure compared to those in polymer films, suggesting a more ordered local environment. Moreover, the orientation times of polar molecules in solvent glasses have been measured to be on the order of seconds, which is much slower than the inverse frequency of the ac Stark field ( $\sim 500$  Hz or 2 ms).<sup>63,64</sup> These observations argue that the relatively low values  $\overline{\Delta\alpha}^{\text{Stark}}$  measured for ATR in the organic glasses may be explained by the fact that neither the ATR nor the solvent molecules of the glass can significantly reorient in response to the field. It is interesting to note that the  $\overline{\Delta\alpha}^{\text{Stark}}$  of ATR in the solvent glasses is somewhat lower than that in rigid polymer films. This has also been seen in electroabsorption measurements of  $\overline{\Delta\alpha}^{\text{Stark}}$  in C153 and is attributed to a residual amount of mobility in the polymers.<sup>26</sup> In the case of C153, this mobility is frozen out by lowering the temperature of the polymers to 77 K and we expect the same would occur for ATR. Because the value of  $\overline{\Delta\alpha}^{\text{Stark}}$  measured in the frozen organic glasses is even lower than  $\overline{\Delta\alpha}_{\text{calc}}$ , we expect that the latter may represent an upper limit to the true value of  $\overline{\Delta\alpha}$  for ATR.

**Other Effects on  $\overline{\Delta\alpha}$ .** Thus far, we have said very little about the effects of vibrational polarizability and/or changes in molecular structure induced by polar solvents on  $\overline{\Delta\alpha}$ . Published work on cyanine dyes has indicated that the solvent field

of the matrix is strong enough to alter the C–C and C=C bond lengths of these molecules, leading to a large effect on both the magnitude and the sign of  $\overline{\Delta\alpha}$ .<sup>19</sup> We expect such changes in bond length to play only a small role in explaining the variation of  $\overline{\Delta\alpha}^{\text{Stark}}$  with matrix polarity observed here for the following reasons. Resonance Raman experiments<sup>55,56</sup> have shown that the C=C and C–C stretching frequencies are only weakly perturbed in solvents with dielectric constants ranging from 2 to 39. The resonance Raman data and calculations in the literature both suggest that the bond length alternation in ATR is not very sensitive to solvent polarity.<sup>12,55,56</sup> Moreover, the solvatochromic dye coumarin 153 exhibits very similar trends in its values of  $\overline{\Delta\alpha}^{\text{Stark}}$  and  $|\Delta\mu|$  in PE and PMMA matrices to those described here.<sup>26</sup> However, the polycyclic aromatic coumarin molecule would *not* be expected to exhibit the large solvent-induced ground-state bond length changes observed in many D–A polyenes.

Addressing the issue of vibrational polarizability, we note that calculations and experiments on ATR have demonstrated that vibrational effects can make an important contribution to the ground-state linear polarizability and to higher-order terms.<sup>65</sup> Though we have not included vibrational polarizability contributions in our calculations of  $\overline{\Delta\alpha}^{\text{el}}$ , we emphasize that the good agreement obtained between the measured and calculated values of  $\overline{\Delta\alpha}$  suggests that we have accounted for the dominant contributions. However, we recognize that vibrational polarizability may play a role in some of the smaller deviations seen between experiment and our calculations.

One unavoidable question in understanding trends in the electronic properties of retinals with solvent polarity is the possible role played by the solvent in modulating the relative energies of the  $1B_u$  and the  $2A_g$  or higher lying  $A_g$  states. Such effects, which are accounted for by the higher order terms ( $\beta$ ,  $\gamma$ , etc.) in the polarizability expansion for the  $1B_u$  state, could significantly influence the measured and calculated values of the excited-state polarizability. Excited-state values of  $\beta$  and  $\gamma$  have been calculated for ATR,<sup>48</sup> and, at typical solvent field strengths, their contributions to the excited-state polarizability are estimated to be quite large. However,  $\beta$  and  $\gamma$  are calculated to be of opposite sign so that their overall contributions nearly cancel at the field strengths present in solution environments. The relatively good agreement between  $\overline{\Delta\alpha}^{\text{Stark}}$  and  $\overline{\Delta\alpha}_{\text{calc}}$  for ATR in the rigid matrices supports this observation though the possible contributions of these higher-order effects warrants further investigation.

**Vibronic Structure in Organic Glasses.** Here we discuss the unique finding that the electroabsorption spectra of ATR in the MCH and MeTHF glasses exhibit vibrational structure. While the derivative nature of Stark spectroscopy makes the underlying structure in the absorption spectrum more apparent, suggestions of a vibronic progression can even be seen in the absorption spectra themselves (Figure 3 top). In order to determine the spacings of the vibronic peaks, the positions of the minima of the second derivative of the absorption spectrum were measured. In MCH, the two observed vibrational spacings are similar at  $1570 \pm 35$  and  $1500 \pm 65$   $\text{cm}^{-1}$  (Figure 3b), while in MeTHF, the first spacing is much smaller at  $1470 \pm 45$   $\text{cm}^{-1}$  and the second is larger at  $1590 \pm 60$   $\text{cm}^{-1}$  (Figure 3e). The most obvious assignment of these features is to a progression of the C=C stretch in the excited state. Our results therefore support the conclusions of previous workers that the overall absorption line width of ATR is dominated by a progression in the C=C stretch.<sup>38,66,67</sup>

The vibrational spacings measured in the MCH matrix are similar to those of the C=C mode in the ground state as measured by resonance Raman,<sup>56,68,69</sup> suggesting a small change in bond order in the excited state. However, in the MeTHF matrix, the marked *decrease* in the frequency of the first C=C stretching band that is observed is evidence that a greater change in excited-state bond order occurs in a more polar environment. A similar trend in the vibronic spacings of the excited-state C=C stretch was observed by Kamalov et al. for bR in poly(vinyl alcohol) films at 10 K.<sup>38</sup> For that system, the vibrational spacings were reported to increase from a value of  $\sim 1200\text{ cm}^{-1}$  to one of  $\sim 1457\text{ cm}^{-1}$  with increasing excitation frequency. Moreover, in bR, a substantial decrease in the frequency of the C=C mode in the Franck–Condon region<sup>38</sup> relative to that in the ground state<sup>70</sup> is observed. The effect of polarity on C=C stretching frequency in ATR and its Schiff base will be the subject of a further communication from this laboratory.

The average fwhm for the vibrational peaks in the two glasses are  $730 \pm 100$  and  $870 \pm 130\text{ cm}^{-1}$  in MCH and MeTHF, respectively. Naturally, we cannot discriminate between homogeneous and inhomogeneous contributions to the line width based on this experiment alone. Nonetheless, these measurements should represent an *upper limit* to the homogeneous broadening of ATR in glassy solvents as our excitation bandwidth is on the order of the line widths we are reporting. We note that these values are in the range reported for the homogeneous line width of ATR in solution that are based on the simultaneous modeling of both the resonance Raman intensities and the absorbance spectra of ATR in room temperature cyclohexane.<sup>66,67</sup> For comparison, note that the line widths of these vibronic bands are similar to the homogeneous line width of the protonated SB form of ATR in bR reported by El-Sayed and co-workers<sup>38</sup> and that of Lee et al.<sup>71</sup> though they are somewhat smaller than that reported by Loppnow et al. in ref 72. Future experiments are planned using narrower excitation widths that should allow us to refine our estimate of the homogeneous width of this system.

## Conclusions

Agreement between the values of  $\overline{\Delta\alpha}^{\text{Stark}}$  and  $\overline{\Delta\alpha}_{\text{calc}}$  is attained for ATR when the matrix containing the probe molecules is sufficiently rigid to prevent reorientation of ATR or matrix molecules in the Stark field. These data demonstrate that the electronic contribution to  $\overline{\Delta\alpha}^{\text{Stark}}$  is  $\sim 50\text{ \AA}^3$  while that due to orientational motion can be as large as  $1000\text{ \AA}^3$ . Likewise, the measured  $|\Delta\mu|$  of ATR ranges from roughly 3 to 12 D, depending on the polarity and the rigidity of the environment. We have put forward the possibility that rotation of the probe molecule causes a decrease in the effective  $|\Delta\mu|$  coupled to an increase in  $\overline{\Delta\alpha}^{\text{Stark}}$ . The vibrational structure of the Franck–Condon region of ATR is resolved for what we believe to be the first time, due to the rigidity of the solvent glass matrices. A progression in the C=C stretch is seen with a vibrational spacing  $\sim 50\text{--}70\text{ cm}^{-1}$  lower than that of the ground state. This demonstrates that the derivative nature of Stark spectroscopy can also be exploited to highlight vibrational progressions in a poorly resolved absorption spectrum.

**Acknowledgment.** We acknowledge the Center for Molecular Analysis at Carnegie Mellon University for the use of the Perkin-Elmer UV–vis spectrometer. We also thank Dr. David Yaron and Dr. Hyung Kim for useful discussions regarding this manuscript and Dr. Zhigang Shuai for INDO/MRD/SDCI sum-over-states calculations of the ground- and excited-state polar-

izabilities of ATR. We also thank our sources of funding: The Winters Foundation, the Petroleum Research Fund administered by the American Chemical Society, and the NSF POWRE and CAREER programs.

## Appendix

Here we summarize the notation used in the paper.

$\Delta\mu$ : The difference in dipole moment between the ground and excited states of the molecule.

$\Delta\mu_{\text{calc}}$ : The value of  $\Delta\mu$  that is calculated using electronic structure methods. This value is corrected for the effects of solvation using both reaction and cavity field models.

$|\Delta\mu|$ : The absolute value of  $\Delta\mu$ . This is the quantity measured in Stark spectroscopy on randomly oriented molecules.

$\Delta\alpha$ : The average value of the change in polarizability between the ground and excited states of the molecule.

$\overline{\Delta\alpha}^{\text{Stark}}$ : The value of  $\overline{\Delta\alpha}$  measured experimentally using Stark spectroscopy.

$\overline{\Delta\alpha}^{\text{el}}$ : The portion of  $\overline{\Delta\alpha}^{\text{Stark}}$  that is attributable to the *electronic* polarizability of the molecule.

$\Delta\alpha_{\text{calc}}$ : The value of the electronic  $\overline{\Delta\alpha}$  that is calculated using electronic structure methods. This value is corrected for the effects of solvation using both reaction and cavity field models.

## References and Notes

- (1) Lewis, A.; Spoonhower, J.; Bogomolni, R. A.; Lozier, R. H.; Stoerkenius, W. *Proc. Natl. Acad. Sci. U.S.A.* **1974**, *71*, 4462–4466.
- (2) Nakanishi, K.; Balough-Nair, V.; Arnaboldi, M.; Tsujimoto, K.; Honig, B. *J. Am. Chem. Soc.* **1980**, *102*, 7945–7947.
- (3) Mathies, R. A.; Lin, S. W.; Ames, J. B.; Pollard, W. T. *Annu. Rev. Biophys. Biophys. Chem.* **1991**, *20*, 491–518.
- (4) Gottfried, D. S.; Steffen, M. A.; Boxer, S. G. *Biochim. Biophys. Acta* **1991**, *1059*, 76–90.
- (5) Sklar, L. A.; Hudson, B. S.; Petersen, M.; Diamond, J. *Biochemistry* **1977**, *16*, 813–819.
- (6) Gottfried, D. S.; Steffen, M. A.; Boxer, S. G. *Science* **1991**, *251*, 662–665.
- (7) Hendrickx, E.; Clays, K.; Persoons, A.; Dehu, C.; Bredas, J. L. *J. Am. Chem. Soc.* **1995**, *117*, 3547–3555.
- (8) Birge, R. R.; Zhang, C.-F. *J. Chem. Phys.* **1990**, *92*, 7178–7195.
- (9) Clays, K.; Hendrickx, E.; Triest, M.; Verbiest, T.; Persoons, A.; Dehu, C.; Bredas, J.-L. *Science* **1993**, *262*, 1419–1422.
- (10) Oudar, J. L.; Chemla, D. S. *J. Chem. Phys.* **1977**, *66*, 2664–2668.
- (11) Marder, S. R.; Gorman, C. B.; Meyers, F.; Perry, J. W.; Bourhill, G.; Bredas, J.-L.; Pierce, B. M. *Science* **1994**, *265*, 632–635.
- (12) Hendrickx, E.; Dehu, C.; Clays, K.; Bredas, J. L.; Persoons, A. In *Polymers for Second-Order Nonlinear Optics*; Lindsay, G. A., Singer, K. D., Eds.; American Chemical Society: Washington, DC, 1995; Vol. 601, pp 82–94.
- (13) Locknar, S. A.; Peteanu, L. A. *J. Phys. Chem. B* **1998**, *102*, 4240–4246.
- (14) Ponder, M.; Mathies, R. *J. Phys. Chem.* **1983**, *87*, 5090–5098.
- (15) Davidsson, A.; Johansson, L. B. *J. Phys. Chem.* **1984**, *88*, 1094–1098.
- (16) Locknar, S. A.; Peteanu, L. A.; Shuai, Z. *J. Phys. Chem. A* **1999**, *103*, 2197–2201.
- (17) Siebold, K.; Navangul, H.; Labhart, H. *Chem. Phys. Lett.* **1969**, *3*, 275–279.
- (18) Bublitz, G. U.; Ortiz, R.; Runser, C.; Fort, A.; Barzoukas, M.; Marder, S. R.; Boxer, S. G. *J. Am. Chem. Soc.* **1997**, *119*, 2311–2312.
- (19) Bublitz, G. U.; Ortiz, R.; Marder, S. R.; Boxer, S. G. *J. Am. Chem. Soc.* **1997**, *119*, 3365–3376.
- (20) Wortmann, R.; Elich, K.; Liptay, W. *Chem. Phys.* **1988**, *124*, 395–409.
- (21) Liptay, W.; Wortmann, R.; Bohm, R.; Detzer, N. *Chem. Phys.* **1988**, *120*, 439–448.
- (22) Oh, D. H.; Sano, M.; Boxer, S. G. *J. Am. Chem. Soc.* **1991**, *113*, 6880–6890.
- (23) Orrit, M.; Bernard, J.; Zumbusch, A. *Chem. Phys. Lett.* **1992**, *196*, 595–600.
- (24) Middendorf, T. R.; Mazzola, L. T.; Lao, K.; Steffen, M. A.; Boxer, S. G. *Biochim. Biophys. Acta* **1993**, *1143*, 223–234.

- (25) Shin, Y. K.; Brunschwig, B. S.; Creutz, C.; Sutin, N. *J. Phys. Chem.* **1996**, *100*, 8157–8169.
- (26) Chowdhury, A.; Locknar, S. A.; Premvardhan, L.; Peteanu, L. A. *J. Phys. Chem. A* **1999**, *103*, 9614–9625.
- (27) Poling is a technique employed to align polar molecules doped within a polymer matrix by applying a dc field to the sample while it is held at a temperature above its  $T_g$ , cooling the film and then removing the field. This technique is used often in materials processing to create noncentrosymmetric arrays of polar molecules for use in nonlinear optical devices.
- (28) Myers, A. B.; Birge, R. R. *J. Am. Chem. Soc.* **1981**, *103*, 1881–1885.
- (29) Tallent, J. R.; Birge, J. R.; Zhang, C.-F.; Wenderholm, E.; Birge, R. R. *Photochem. Photobiol.* **1992**, *56*, 935–952.
- (30) Merchan, M.; Gonzalez-Luque, R. *J. Chem. Phys.* **1997**, *106*, 1112–1122.
- (31) Mathies, R.; Stryer, L. *Proc. Natl. Acad. Sci. U.S.A.* **1976**, *73*, 2169–2173.
- (32) Moylan, C. R. *J. Phys. Chem.* **1994**, *98*, 13513–13516.
- (33) McCarthy, P. K.; Blanchard, G. J. *J. Phys. Chem.* **1993**, *97*, 12205–12209.
- (34) Kurtz, H. A. *Int. J. Quantum Chem: Quantum Chem. Symp.* **1990**, *24*, 791–798.
- (35) Kurtz, H. A.; Stewart, J. J. P.; Dieter, K. M. *J. Comput. Chem.* **1990**, *11*, 82–87.
- (36) Ponder, M. C. Ph.D. Thesis, University of California, Berkeley, CA, 1983.
- (37) Birge, R. R.; Bocian, D. F.; Hubbard, L. M. *J. Am. Chem. Soc.* **1982**, *104*, 1196–1207.
- (38) Kamalov, V. F.; Masciangioli, T. M.; El-Sayed, M. A. *J. Phys. Chem.* **1996**, *100*, 2762–2765.
- (39) Bevington, P. R.; Robinson, D. K. *Data Reduction and Error Analysis for the Physical Sciences*, 2nd ed.; McGraw-Hill: New York, 1992; p 328.
- (40) Liptay, W. In *Excited States*; Lim, E. C., Ed.; Academic Press: New York, 1974; pp 129–229.
- (41) During the course of this study, we discovered that we had previously neglected to normalize the absorption spectrum derivatives to the light frequency. This omission in the earlier work accounts for the discrepancy between eq 1 in ref 13 and in this paper, and for the differences between the values reported for ATR in glued PMMA in both sources. The effect on  $\Delta\alpha$  and  $|\Delta\mu|$  is small (<10% and <20%, respectively) and the trends we have observed are not affected by this oversight.
- (42) Dewar, M. J. S.; Zoebisch, E. G.; Healy, E. F.; Stewart, J. J. P. *J. Am. Chem. Soc.* **1985**, *107*, 3902–3909.
- (43) Hamanaka, T.; Mitsui, T.; Ashida, T.; Kakudo, M. *Acta Crystallogr.* **1972**, *B28*, 214–222.
- (44) Premvardhan, L.; Peteanu, L. *Chem. Phys. Lett.* **1998**, *298*, 521–529.
- (45) Bottcher, C. J. F. *Theory of Electric Polarisation*; Elsevier Publishing Co.: Amsterdam, 1952; p 492.
- (46) Sakurai, M.; Ando, I.; Inoue, Y.; Chujo, R. *Photochem. Photobiol.* **1981**, *34*, 367–374.
- (47) Bublitz, G. U.; Boxer, S. G. *J. Am. Chem. Soc.* **1998**, *120*, 3988–3992.
- (48) Shuai, Z., personal communication.
- (49) Birge, R. R.; Bennett, J. A.; Hubbard, L. M.; Fang, H. L.; Pierce, B. M.; Kliger, D. S.; Leroi, G. E. *J. Am. Chem. Soc.* **1982**, *104*, 2519–2525.
- (50) Liess, M.; Jeglinski, S.; Vardeny, Z. V.; Ozaki, M.; Yoshino, K.; Ding, Y.; Barton, T. *Phys. Rev. B* **1997**, *56*, 15712–15724.
- (51) For instance, if  $\epsilon_0$  in both MCH and MeTHF increased by 10 units to 12 and 14.6, respectively,  $\Delta\mu_{\text{calc}}$  values would increase to 8.3 and 8.4 D, respectively, and  $\Delta\alpha_{\text{calc}}$  values would increase to 82 and 83 Å<sup>3</sup>, respectively.
- (52) Although most commercial low-density polyethylene at room temperature contains both amorphous and crystalline regions, recent fluorescence studies on tethered pyrene molecules (Zimmerman, O. E.; Weiss, R. G. *J. Phys. Chem. A* **1998**, *102*, 5364–5374) indicate that probe molecules inhabit the amorphous or interfacial (between crystalline and amorphous) regions of the film.
- (53) An unrealistically large contraction of 20% for all three elliptical axes caused an increase in both  $\Delta\mu_{\text{calc}}$  and  $\Delta\alpha_{\text{calc}}$  of roughly 10% in cold versus room temperature PE.
- (54) One could argue at this point that the effects we observe in ATR are simply the result of isomerizations of the molecule. However, calculations of both  $\Delta\mu$  and  $\Delta\alpha$  performed on 13- and 9-*cis*-retinal differ from that of ATR by only 15%. This small deviation would hardly account for the large variations seen here. Also, ATR is the most stable isomer. In solutions of ATR irradiated for 2 h in hexane at 430 nm, ATR formed at least 60% of the mixture at equilibrium (Waddell, W. H.; Hopkins, D. L. *J. Am. Chem. Soc.* **1977**, *99*, 6457–6459).
- (55) Locknar, S. A.; Peteanu, L. A., manuscript in preparation.
- (56) Heyde, M. E.; Gill, D.; Kilponen, R. G.; Rimai, L. *J. Am. Chem. Soc.* **1971**, *93*, 6776–6780.
- (57) Saal, S.; Haase, W. *Chem. Phys. Lett.* **1997**, *278*, 127–132.
- (58) Diezemann, G. *J. Chem. Phys.* **1997**, *107*, 10112–10120.
- (59) Rossler, E. *Phys. Rev. Lett.* **1990**, *65*, 1595–1598.
- (60) Ediger, M. D.; Angell, C. A.; Nagel, S. R. *J. Phys. Chem.* **1996**, *100*, 13200–13212.
- (61) Ferry, J. D. *Viscoelastic Properties of Polymers*, 1st ed.; John Wiley & Sons: New York, 1961; Chapter 16.
- (62) Van Krevelen, D. W. *Properties of Polymers*, 3rd ed.; Elsevier: Amsterdam, 1997.
- (63) Rossler, E.; Sillescu, H. *Chem. Phys. Lett.* **1984**, *1984*, 94–98.
- (64) Richert, R. *Chem. Phys. Lett.* **1993**, *216*, 223–227.
- (65) Zuliani, P.; DelZoppo, M.; Castiglioni, C.; Zerbi, G.; Marder, S. R.; Perry, J. W. *J. Chem. Phys.* **1995**, *103*, 9935–9940.
- (66) Myers, A. B.; Trulson, M. O.; Pardo, J. A.; Heeremans, C.; Lugtenburg, J.; Mathies, R. A. *J. Chem. Phys.* **1986**, *84*, 633–640.
- (67) Myers, A. B. Ph.D. Thesis, University of California at Berkeley, 1984.
- (68) Locknar, S. A.; Peteanu, L. A., manuscript in preparation.
- (69) Curry, B.; Broek, A.; Lugtenburg, J.; Mathies, R. A. *J. Am. Chem. Soc.* **1982**, *104*, 5274–5286.
- (70) Mathies, R. A. *Methods Enzymol.* **1982**, *88*, 633–643.
- (71) Lee, I.-J.; Gillie, J. K.; Johnson, C. K. *Chem. Phys. Lett.* **1989**, *156*, 227–232.
- (72) Loppnow, G. R.; Mathies, R. A.; Middendorf, T. R.; Gottfried, D. S.; Boxer, S. G. *J. Phys. Chem.* **1992**, *96*, 737–745.
- (73) Lide, D. R. *Handbook of Chemistry and Physics*, 71 ed.; CRC Press: Boca Raton, FL 1990–1991.
- (74) Greenspan, H.; Fischer, E. *J. Phys. Chem.* **1965**, *69*, 2466–2469.